Correlating Precipitation Dynamics with Land-use Land-cover change over Mahanadi River Basin in India

Rajput Preeti[1,2*], Verma Mukesh Kumar[3], Garg Ajay Kumar[1] and Sinha Manish Kumar[2]
1. Department of Civil Engineering, Government Engineering College Raipur, Raipur-492015, Chhattisgarh, INDIA
2. Department of Environmental and Water Resources Engineering, University Teaching Department, Chhattisgarh Swami Vivekanand Technical University Bhilai, Bhilai-491107, Chhattisgarh, INDIA
3. Department of Civil Engineering, National Institute of Technology Raipur, Raipur-492001, Chhattisgarh, INDIA
*preetisse@gmail.com

Abstract

The pattern of precipitation has shifted over time, shaped by alterations in land use and land cover (LULC), which impacted local meteorological conditions. This study analyzes LULC changes in the Mahanadi River basin, utilizing satellite observations and meteorological reanalysis datasets to assess their impact on regional weather parameters and surface fluxes. The impact of LULC changes on regional meteorology was investigated by applying correlation analysis with multiple linear regression to weather variables. The objective was to ascertain the enduring relationship between precipitation and atmospheric heat, as well as to quantify these dynamics in Aw and Cwa climate zones throughout both monsoon and non-monsoon seasons. Landsat TM and ETM+ satellite imagery was used to produce LULC data for the years 2005, 2010, 2015 and 2020. Over the previous 20 years, plantation lands fell 69%, according to LULC change statistics, whereas built-up and agricultural areas grew by 11% and 21% respectively. Correlation analysis indicates that the R^2 value between precipitation and relative humidity varies from 0.70 to 0.78. The Bowen ratio and solar radiation have an inverse connection with precipitation, with R^2 values ranging from 0.5 to 0.6 and 0.7 to 0.8, respectively, indicating that lessened latent heat and elevated solar radiation are associated with decreased precipitation.

According to the results, more impermeable surfaces will lower the amount of water in the atmosphere. This will cause solar energy and the Bowen ratio to rise, while humidity in the air will decrease. The research emphasizes significant alterations in climatic conditions and surface fluxes, leading to atmospheric heat and reduced moisture levels. These findings highlight the significance of proficient LULC management in alleviating these effects.

Keywords: Bowen ratio, Latent heat, Mahanadi River basin, Multiple linear regression, Relative humidity, Sensible heat.

Introduction

An essential component of the climate system of the Earth is the cycling of heat flux and moisture in the atmosphere which has a considerable impact on the energy budget of the atmosphere. The partitioning of solar energy into latent heat and sensible heat is a significant function of land cover which plays a crucial role in the regulation of water and energy exchanges between the land and the atmosphere[18]. In order to understand the variability of precipitation across landscapes, it is necessary to conduct measurements on a regional scale across all sorts of land cover environments. The transformation of solar energy at the surface of the ground into latent heat (evaporation) and sensible heat is a major process in the climate system[1]. It is also a primary factor that controls the terrestrial component of the hydrological cycle.

In recent years, there has been an increasing interest in utilizing land use management as a means to enhance both local precipitation and climatic services[20]. Besides the influence of latent heat (evaporation) on water availability, sensible heat can regulate near-surface temperature, particularly when energy balance partitioning at the land surface significantly affects atmospheric conditions[16]. The variability of flux partitioning and the factors that influence it, has, however, been the subject of very few investigations up to this point[19]. This study emphasizes the dynamics and determinants of precipitation instead of examining land surface-atmosphere exchange systems[10].

Beginning with the primary emphasis on energy constraint as a catalyst for precipitation, recent observations have highlighted the application of the Bowen ratio approach to examine the impact of water limitation on precipitation reduction[14]. The two-dimensional precipitation restriction concept, which posits that precipitation is restricted by the availability of water and energy, currently serves as the prevalent framework for presenting and categorizing the determinants of precipitation[23]. The continuously fluctuating precipitation data underscores the necessity to assess the existing framework and to persist in examining energy partitioning and precipitation determinants across various scales, weather conditions and land cover types[20].

The transport mechanism may be regarded as a term of mechanical energy; it may also be viewed as an efficiency term governing the exchange processes of energy and water between the land surface and the atmosphere. The effectiveness of this exchange may vary in strength, hence clarifying a portion of the diversity in precipitation[19]. This indicates that exchange efficiency may be regarded as a third dimension, alongside energy availability and water

availability, to elucidate precipitation dynamics across various land cover types[4]. Consequently, the examination of the dynamics and determinants of precipitation across various land cover types is organized along three dimensions: energy availability, water availability and exchange efficiency.

To describe the determinants of precipitation within a three-dimensional framework, where precipitation may be constrained by energy availability, water availability, or exchange efficiency, the input variables are categorized accordingly. The nine potential determinant variables considered in the analysis are categorized as follows:

- **Energy availability:** Net solar radiation (SR), Latent heat (LH), sensible heat (SH), Bowen ratio (BR)
- **Water availability:** Soil Moisture (SM), Evaporation (EV), Precipitation (TP)
- **Exchange efficiency:** Wind Speed (WS), Relative Humidity (RH), 2-Meter Temperature (TE)

This study offers an initial synthesis of the factors influencing precipitation dynamics across intricate landscapes, articulated as a three-dimensional framework where precipitation is constrained by energy availability, water availability, or exchange efficiency, based upon land cover. The concept of a three-dimensional limiting system is not novel, as it parallels the fire triangle where heat, fuel and oxygen dictate the circumstances necessary for the existence of fire[11]. The absence of any of these ingredients will result in the absence of fire. Similar to the fire triangle, the location of a site with a specific land cover type within the 'precipitation triangle' determines whether the system is predominantly constrained by energy availability, water availability, or exchange efficiency.

For the purpose of this study, the data-driven analysis focuses entirely on the conventional meteorological variables. It can therefore be understood as a statistical analysis of the correlation between precipitation and the meteorological drivers[23], rather than a causal description of the mechanisms that link the meteorological drivers to precipitation through the involvement of vegetation. The findings of this research have the potential to contribute to a better understanding of the dynamics of precipitation across a variety of land cover types. Additionally, they may assist in optimizing and maybe simplifying models that are used to predict precipitation.

Material and Methods

This study examines the Mahanadi River basin in India, situated from 19° 21' N to 23° 35' N latitude and 80° 30' E to 86° 50' E longitude, distinguished by its monsoon-influenced humid subtropical climate (Cwa) and tropical wet and dry climate (Aw)[26]. The Mahanadi is an interstate river in eastern India, traversing the State of Chhattisgarh and Odisha. The basin's catchment region includes significant portions of Chhattisgarh and Odisha, comprising, approximately 52% and 46% of the total basin area respectively. The Mahanadi River basin has diverse topography, with the lowest elevation located in the coastal areas and the highest elevation in the northern hills[21]. A significant percentage of the alluvial region of the Mahanadi basin is situated within the 200-400 m elevation range.

The maximum relative humidity in the basin ranges from 68% to 87%. A significant portion of the basin area receives 1200-1400 mm of precipitation, with certain regions recording nearly 1600 mm, resulting in an average annual basin rainfall of approximately 1292 mm. Over 90% of the annual precipitation transpires during the monsoon season. The predominant soil types in the basin include red and yellow soils, mixed red and black soils, laterite soils and deltaic soils[24]. Spatiotemporal assessments of precipitation variability have been conducted utilizing 83 years (1940–2023) of monthly high-resolution gridded datasets at a 0.25° x 0.25° scale. ERA-5 is a comprehensive long-term global atmospheric reanalysis dataset generated by the European Centre for Medium-Range Weather Forecasts (ECMWF).

Among the numerous reanalysis datasets, ERA-5 exhibits values that closely align with those recorded by IMD. Significant correlations have been detected between the IMD and ERA-5 reanalysis datasets. Numerous investigations into several aspects of Indian precipitation have been conducted utilizing these high-resolution gridded datasets. In this study, the role of land cover in determining the drivers of precipitation with respect to weather parameters is investigated by comparing sites of different types of land cover that are located within the same region and climatic setting. This is accomplished with the assistance of Pearson cross correlation and multiple linear regression analysis.

An analysis of land cover change has been conducted in the Mahanadi basin for the years 2005, 2010, 2015 and 2020 to comprehend the variability in precipitation associated with changes in land use and land cover[28]. Digital image processing techniques were employed to analyze satellite images and extract meaningful information. Process of image categorization was carried out on images that have several spectral components. The Landsat images that were georeferenced to the Universal Traverse Mercator (UTM) projection system, zone 44 N, with datum WGS 84, were downloaded and used for the analysis. The maximum likelihood method is employed for supervised classification within the ERDAS Image processing software[29].

This method classifies all image pixels into distinct land cover categories according to their comparable digital number (DN) values[9]. Evaluating the precision of digital image classification results is crucial. The Kappa coefficient is calculated for the chosen sampling points to perform an accuracy assessment. The land use and land cover were categorized into six distinct classes: Water Body, Built-up, Forest, Agriculture, Plantation and Waste land.

To illustrate the findings for the complete Mahanadi River basin, two sites for each category of land use and land cover in both climates (Cwa and Aw) were selected. The correlation analysis has been conducted for the selected points in the 83-year monthly dataset time series. For each site, the following variables were utilized to examine the factors influencing precipitation: Net solar radiation (SR)[30], Latent Heat (LH)[1], Sensible Heat (SH)[5], Wind Speed (WS)[2], Relative Humidity (RH)[27], Precipitation (TP)[15], Bowen ratio (BR)[14], Temperature (TE)[6] and Soil moisture (SM)[3] based on literature reviews[25]. These variables are organized into three subsets: energy availability, water availability and exchange efficiency.

A regression analysis incorporating nine input variables was conducted to gain insight into the dynamics of precipitation at each site. By employing a regression method, researcher arrive at conclusions that are based on the data rather than relying on assumptions that are based on the process[22]. In this analysis, all input variables were standardized to fall within the range of 0 to 100. Additionally, the regression method necessitates the availability of all variables at each timestep. If a value is missing, the corresponding timestep is eliminated from the dataset. Moreover, it is essential that each input variable maintains temporal independence. While conducting an analysis of environmental variables through time series, it was observed that the temporal dependence within the data is not particularly robust[12].

To address multicollinearity in the regression equation, one of the predictor variables would be excluded from the subset selection method if it exhibited a cross-correlation exceeding 0.7 with other variables[13]. All potential multiple linear regression equations are delineated with the structure specified as:

$$Y = \beta_0 + \beta_1 X_1 + \beta_2 X_2 + \ldots + \beta_i X_i + \epsilon \quad (1)$$

where Y represents the dependent variable, X_i denotes the explanatory variable(s), β_0 is the intercept, β_i signifies the parameter(s) and ϵ stands for the error term. The optimal equations for each subset size are identified from all potential subsets, utilizing objective statistical criteria, specifically Mallow's C_p value in this study.

To determine whether each predictor in the model is statistically significantly contributing to the explanation of the dependent variable's dynamics, the best regression equation identified by the subset selection approach was tested for Variance Inflation Factors (VIF). The generated model coefficients show the relative contribution of each predictor in describing the dynamics of precipitation because the input data was normalized[31]. For the multiple linear regression model predictors' coefficients to add up to 100, they were standardized. The objective was to articulate the factors influencing precipitation within a three-dimensional context, where precipitation may be constrained by energy availability, water availability, or exchange efficiency. The input variables are categorized accordingly. The coefficients of the regression equation predictors are aggregated by category, thereby offering insights into the relative contribution of each category in identifying the dynamics of precipitation.

The total summation of the coefficients amounting to 100 does not imply that the regression equation accounts for 100% of the variance in precipitation dynamics; instead, it serves to illustrate the relative contributions of the three limitation categories. To provide an explanation for the dynamics of the precipitation, the entire technique of regression analysis was carried out for the precipitation as the dependent variable as well, employing the same categories of independent factors. This study employs the regression method to investigate the relative contributions of the three groups of variables in accounting for the variance of precipitation at each observed site. The results are illustrated through a ternary plot where each of the three axes corresponds to a set of variables associated with energy availability, water availability and exchange efficiency, respectively.

Results and Discussion

LULC change analysis of Mahanadi River basin: The Mahanadi basin's landscape is anthropogenically managed, creating a mosaic of urban centers, forests, wastelands, agricultural land, plantations and water bodies in proximity. Diverse land utilization results in alterations to land cover. Landsat TM and ETM+ satellite imagery were utilized to generate LULC data for the years 2005, 2010, 2015 and 2020 and to ascertain the associated changes. Figure 1 illustrates the LULC maps for the years 2005, 2010, 2015 and 2020. The dynamic characteristics of various land use types reveal substantial alterations in the distinct LULC classes of the studied area. The maximum likelihood method was applied in ERDAS image processing software to analyze satellite images with a high degree of accuracy (87.75% Kappa Coefficient). Four LULC maps were produced for the research region as a result of the analysis of the images.

The generated maps indicated that the predominant portion of the LULC within the research area is comprised of agricultural land, estimated at 43% in 2005, 51% in 2015 and 52% in 2020, reflecting a cumulative increase of 21% from 2005 to 2020 (Figure 2). Forest coverage has been stable with minimal variation over the past 15 years, encompassing 32% of the overall study area. The extent of built-up area is minimal, although it gradually increases over time, exhibiting an 11% growth from 2005 to 2020. The statistical analysis of land coverage reveals a decline in plantation (12% coverage), wasteland (6% coverage) and waterbody (5% coverage) at a temporal resolution of 15-year intervals, with total changes of 69%, 25% and 2% respectively. Table 1 illustrates the spatial extent of several land use categories. In summary, plantations undergo the most significant alteration, followed by changes in agriculture and wasteland.

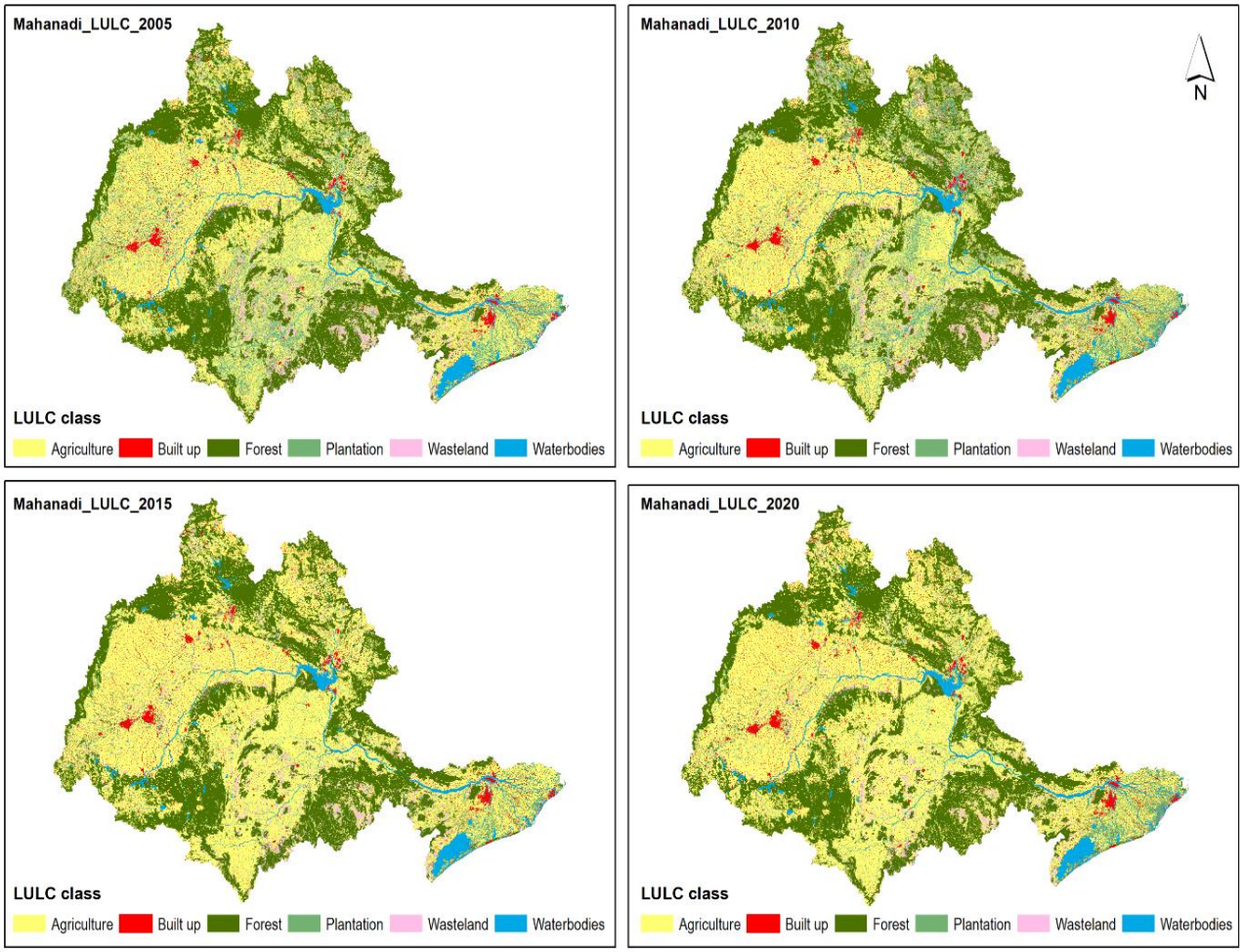

Figure 1: Class wise LULC of Mahanadi basin for year 2005, 2010, 2015 and 2020

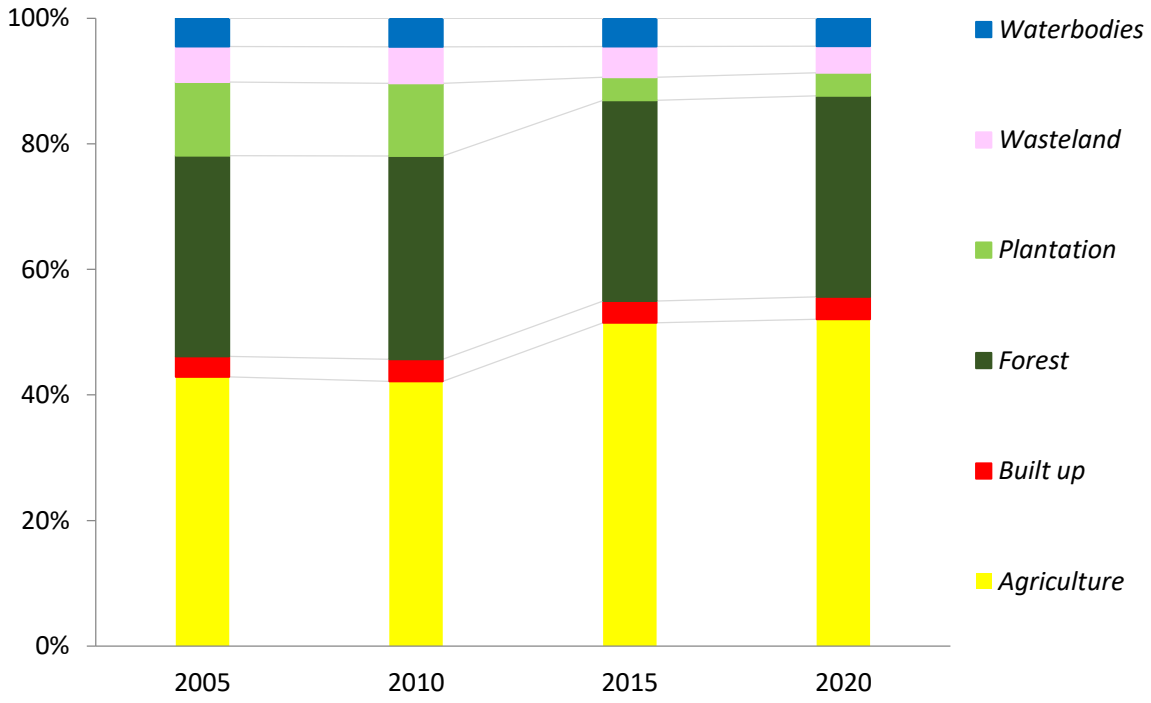

Figure 2: Year wise percentage change of LULC class of Mahanadi basin

https://doi.org/10.25303/187da014024

Table 1
Land use land cover class (area in Kms) of Mahanadi River basin and total percentage change in individual LULC class in last 15 years

Year → / Class ↓	2005	2010	2015	2020	Total Change
Agriculture (AG)	62066.7	62223.9	74571.2	75317.5	21%
Built up (BU)	4795.78	5050.22	5069.18	5342.98	11%
Forest (FO)	46272.38	46259.87	46269.95	46309.43	0%
Plantation (PL)	17001.99	16510.9	5304.13	5346.34	69%
Wasteland (WL)	8161.39	8276.46	7125.36	6105.33	25%
Waterbodies (WB)	6519.96	6496.81	6478.34	6396.57	2%

Table 2
Correlation coefficient values of Bowen ratio, Relative Humidity and Solar Radiation with Precipitation

Climate Zone	LULC Class	BR	RH	SR	Climate Zone	LULC Class	BR	RH	SR
Aw	Agriculture	-0.51	0.69	-0.72	Cwa	Agriculture	-0.54	0.73	-0.68
	Built up	-0.61	0.75	-0.73		Built up	-0.54	0.78	-0.71
	Forest	-0.59	0.75	-0.75		Forest	-0.51	0.74	-0.67
	Plantation	-0.53	0.77	-0.78		Plantation	-0.55	0.79	-0.71
	Wasteland	-0.59	0.78	-0.80		Wasteland	-0.56	0.77	-0.74
	Waterbodies	-0.49	0.70	-0.71		Waterbodies	-0.56	0.76	-0.69

Correlation between precipitation and weather variables: The study investigates land use and land cover change, along with the corresponding modifications in surface-level meteorology. It analyzes the variation in total precipitation in relation to weather variables such as relative humidity, solar radiation, latent heat, sensible heat, wind speed, evaporation, soil moisture and temperature, utilizing ERA5 reanalysis datasets across six distinct land use and land cover classes.

To analyze the relationship between precipitation and local weather variables, Pearson correlation coefficients are computed for both climate zones (Cwa and Aw) across various land use and land cover classes. To derive significant insights from the analysis, the selection of variables was conducted by constraining the correlation values among them. Only the correlation values between the variables that exceeded 0.5 were chosen for further analysis. The variable with the highest value of cross-correlation among the variables was selected. Figure 3 illustrates the cross-correlation. Table 2 demonstrates that the Bowen ratio, relative humidity and solar radiation exhibit a significant correlation with precipitation in the dataset under consideration.

The analysis reveals that the Bowen ratio and solar radiation exhibit an inverse correlation, with R2 values ranging from 0.5 to 0.6 and 0.7 to 0.8 respectively. This indicates that lower amounts of latent heat combined with higher solar radiation result in reduced precipitation levels. The relative humidity exhibits a direct correlation with precipitation, indicated by an R2 value ranging from 0.70 to 0.78. To validate this result, time series plots of weather variables were created to observe the relative behavior of the variables under known anomaly conditions. Figure 4 illustrates the time series plot for the month of September spanning from 1970 to 2010. The figure highlights three significant drought events from 1974, 1984 and 1996 to illustrate the cross-correlation between the variables. The time series plot indicates an inverse correlation between the Bowen ratio, solar radiation and temperature with precipitation. Meanwhile, the amount of precipitation is directly proportional to the relative humidity.

This study aims to analyze the long-term relationship between precipitation and atmospheric parameters, quantifying this relationship across various land use and land cover types using a multiple linear regression approach. The principles of atmospheric thermodynamics indicate that the hydrological cycle is significantly influenced by the interactions occurring between land and atmosphere[17]. Consequently, a regression analysis was conducted with three selected input variables to elucidate the dynamics of precipitation across six land use classes within both climate zones utilizing a regression method. In this analysis, all input variables were standardized to fall within a range of 0 to 100.

Additionally, the regression approach necessitates that all variables are present for every timestep. When a value is absent, the corresponding timestep is eliminated from the dataset. Furthermore, it is essential that each input variable exhibits temporal independence. While we are utilizing time series of environmental variables, the autocorrelation analysis indicated that the temporal dependence within the data is weak.

This study utilizes a dataset comprising 83 years of monthly data, spanning from 1940 to 2023. A comprehensive dataset

spanning multiple years including 1941 – 1989, 1961 – 2009, 1981 – 2023 and 1941 – 2023, along with various sites for each land cover type, is utilized to analyse the precipitation regime associated with those land cover types. The variables that can account for a portion of the variance in precipitation may be referred to as drivers, based on the assumption that the system is sensitive and that the drivers themselves are variable and not constant[8]. The input parameters are referred to as drivers when changes in these parameters result in variations in precipitation.

The results obtained are illustrated in figure 5, a ternary plot. In the ternary plot, each of the three axes corresponds to one of the limitation categories: energy availability, water availability and exchange efficiency. The location of a LULC site within the triangle indicates the proportionate impact of each category in describing the variance of precipitation for that specific LULC site.

The relative positioning of these study sites along the three axes indicates that land use and land cover partially account for the variance in precipitation. Research indicates that during the monsoon season, the dynamics of precipitation reveals that energy availability is the primary contributor, with water availability and exchange efficiency following closely behind.

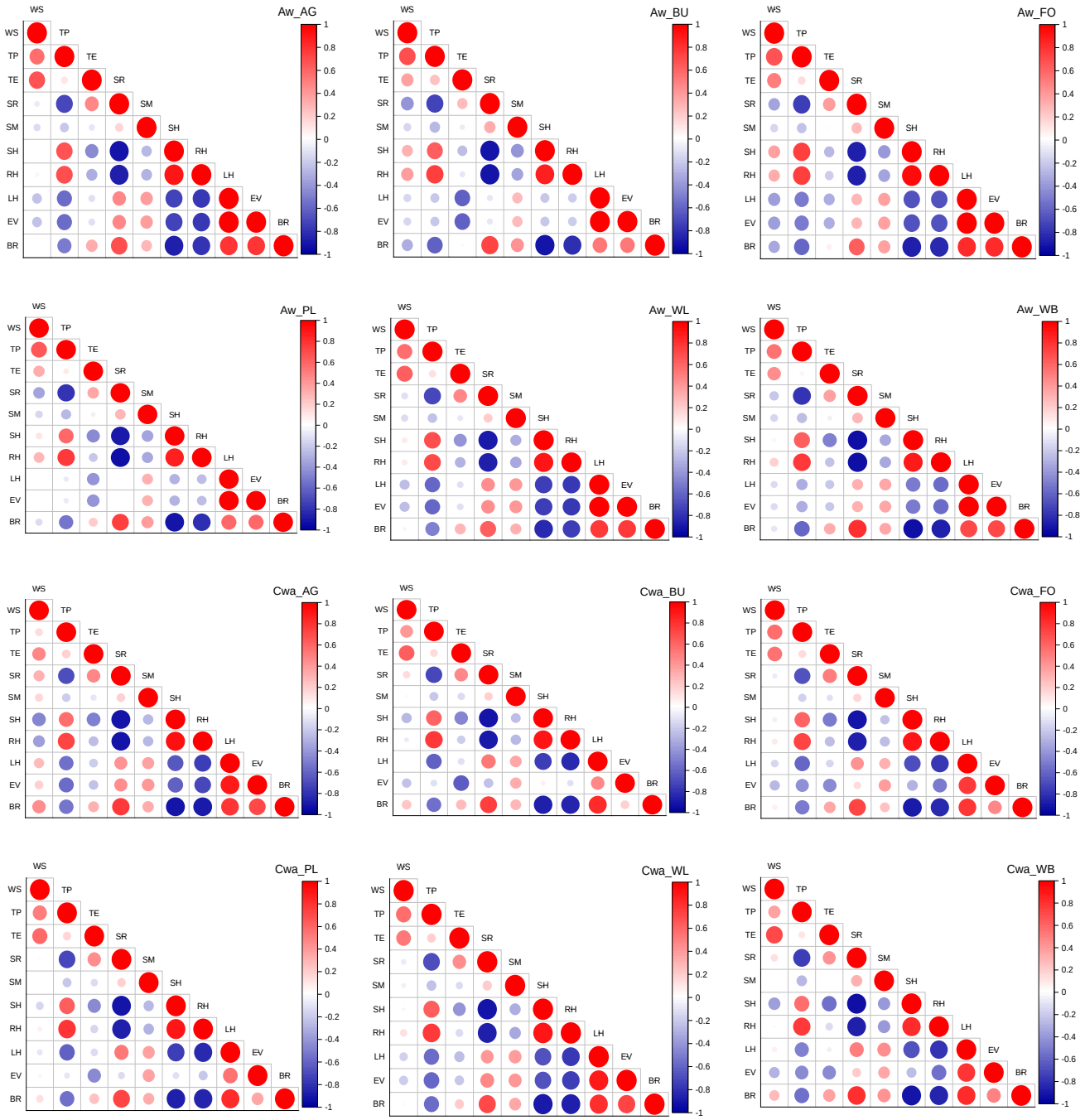

Figure 3: Pearson cross-correlation coefficient between weather variables for individual LULC class and climate zone

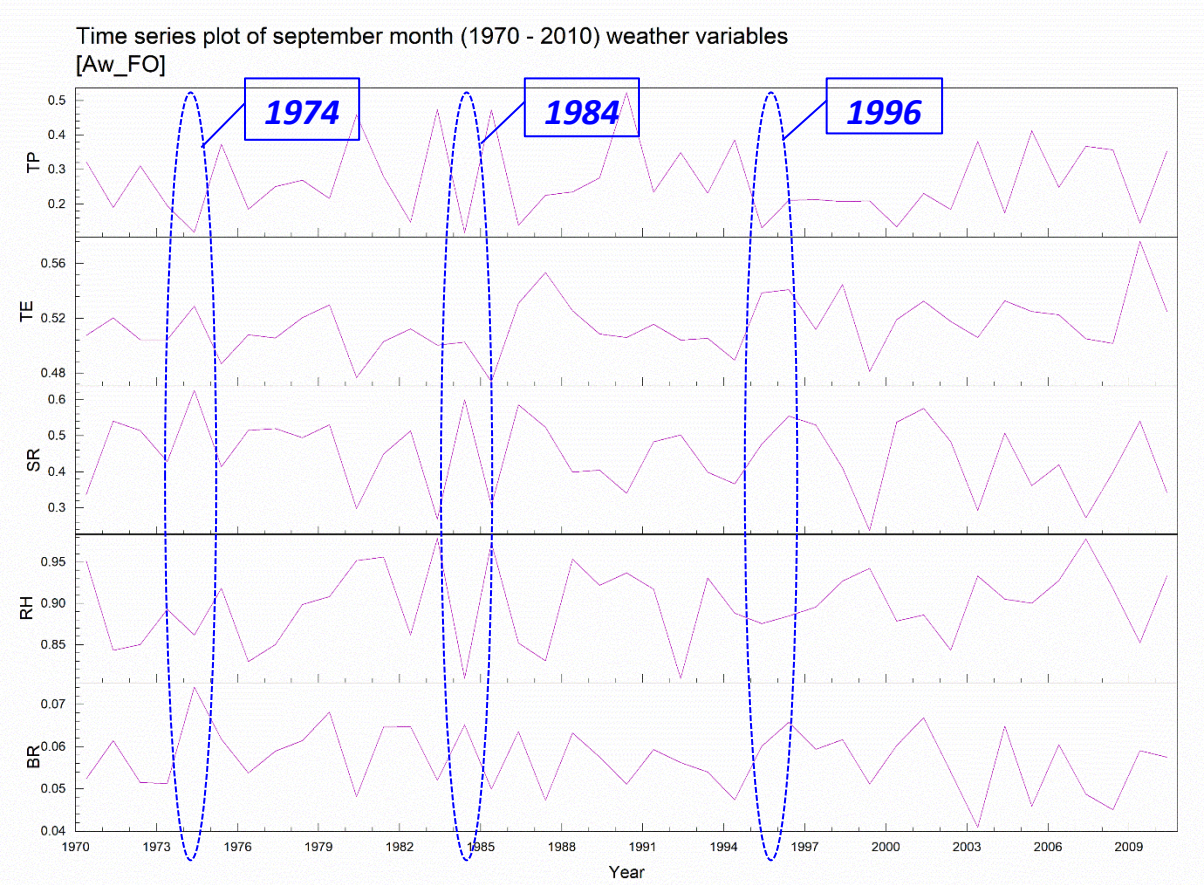

Figure 4: Time series plot of weather variables from 1970 to 2010 (highlighting major drought events)

During the pre-monsoon and post-monsoon seasons, water availability will primarily influence precipitation followed by energy and exchange efficiency contributing in that order.

The analysis of results concerning climate zones indicates that during the monsoon season, the energy contribution in Cwa climates is limited to a range of 40% to 60%, while in Aw climates, it extends over a broader spectrum of 25% to 75%. In the context of pre-monsoon and post-monsoon seasons within a Cwa climate, the variations can be predominantly attributed to water availability. However, in Aw climate, there has been a significant contribution observed in exchange efficiency.

Furthermore, the data indicates that agriculture, forest and waste land exhibit comparable traits regarding the percentage variance of drivers across the three dimensions of energy, water and exchange efficiency. The limitation of exchange efficiency was observed to be most pronounced at the inland water body sites. The precipitation in this type of land cover does not directly correlate with fluctuations in incoming global energy due to its significant heat capacity; instead, it is more directly influenced by atmospheric demand [7]. Additionally, there exist other forms of land cover that face limitations in exchange efficiency, though to a reduced degree. The findings regarding built-up areas indicate that precipitation within these systems is significantly controlled by energy availability. This is associated with the extensive non-porous surfaces found in urban environments.

The distribution of radiation to sensible heat which directly warms the earth's surface and atmosphere, is significantly influenced by latent heat. With the increasing coverage of the earth's surface by pavement, there is a reduction in evaporation rates, leading to an increase in the distribution of net radiation to sensible heat (resulting in a higher Bowen ratio) which subsequently elevates urban temperatures. As a result, the relative humidity in urban environments decreases, a phenomenon referred to as urban dryness similar to the results obtained by Zheng et al[32]. The findings enhance our comprehension of precipitation dynamics across various land cover types and could aid in optimizing and possibly streamlining models for precipitation prediction.

Trend of weather variables: The impacts of LULC changes on atmospheric conditions, weather and climate occur through modifications in land-atmosphere interactions, manifesting at various scales from local and regional to global levels. Therefore, the long-term changes in land use and land cover are significant regarding their effects on weather and climate. To examine the effects of land use and land cover changes on local weather patterns, time series plots of solar radiation, Bowen ratio and relative humidity were created.

The graph in figure 6 illustrating solar radiation and Bowen ratio, shows an inverse correlation with precipitation and reveals an upward trend over the period from 2005 to 2020. That indicates a decline in precipitation over time. The relative humidity exhibits a negative trend, which correlates directly with precipitation. This state shows a declining trend in precipitation over the period from 2005 to 2020.

Conclusion

This research has demonstrated that the water availability axis in the three-dimensional precipitation restriction paradigm does affect LULC sites in the areas of agriculture, waterbodies, forests, plantations and built-up areas. The regression analysis conducted across the three seasons: pre-monsoon, monsoon and post-monsoon indicating that precipitation is primarily constrained by factors such as energy availability, water availability, or exchange efficiency, which vary according to the type of land cover. The inclusion of exchange efficiency in elucidating the precipitation process highlights the transition from the traditional two-dimensional framework which solely accounts for energy and water limitations, to a more comprehensive three-dimensional concept of precipitation limitation.

The integration of data by land cover type indicated that precipitation during the pre-monsoon and post-monsoon seasons for agriculture, forest, wasteland and plantation is primarily characterized as energy-limited. Furthermore, the limitation of exchange efficiency is significant in characterizing the dynamics of precipitation in urban areas. Both exchange efficiency and energy availability are equally important in describing the rest of the precipitation dynamics. The dynamics of forest precipitation can largely be attributed to water availability.

The findings of this analysis are considered appropriate for use as a reference in determining uncertainty ranges for other sites that have shorter monitoring durations. This study aims to analyze the trends in precipitation changes in relation to solar radiation, Bowen ratio and relative humidity along with their underlying causes at a local scale. The variation in relative humidity is affected not just by changes in temperature, but also by fluctuations in the amount of latent heat emanating from the earth's surface. Temperature variations close to the earth's surface primarily result from alterations in thermal exchanges (heat balance) between the earth's surface and the atmosphere, along with shifts in the conditions of the earth's surface.

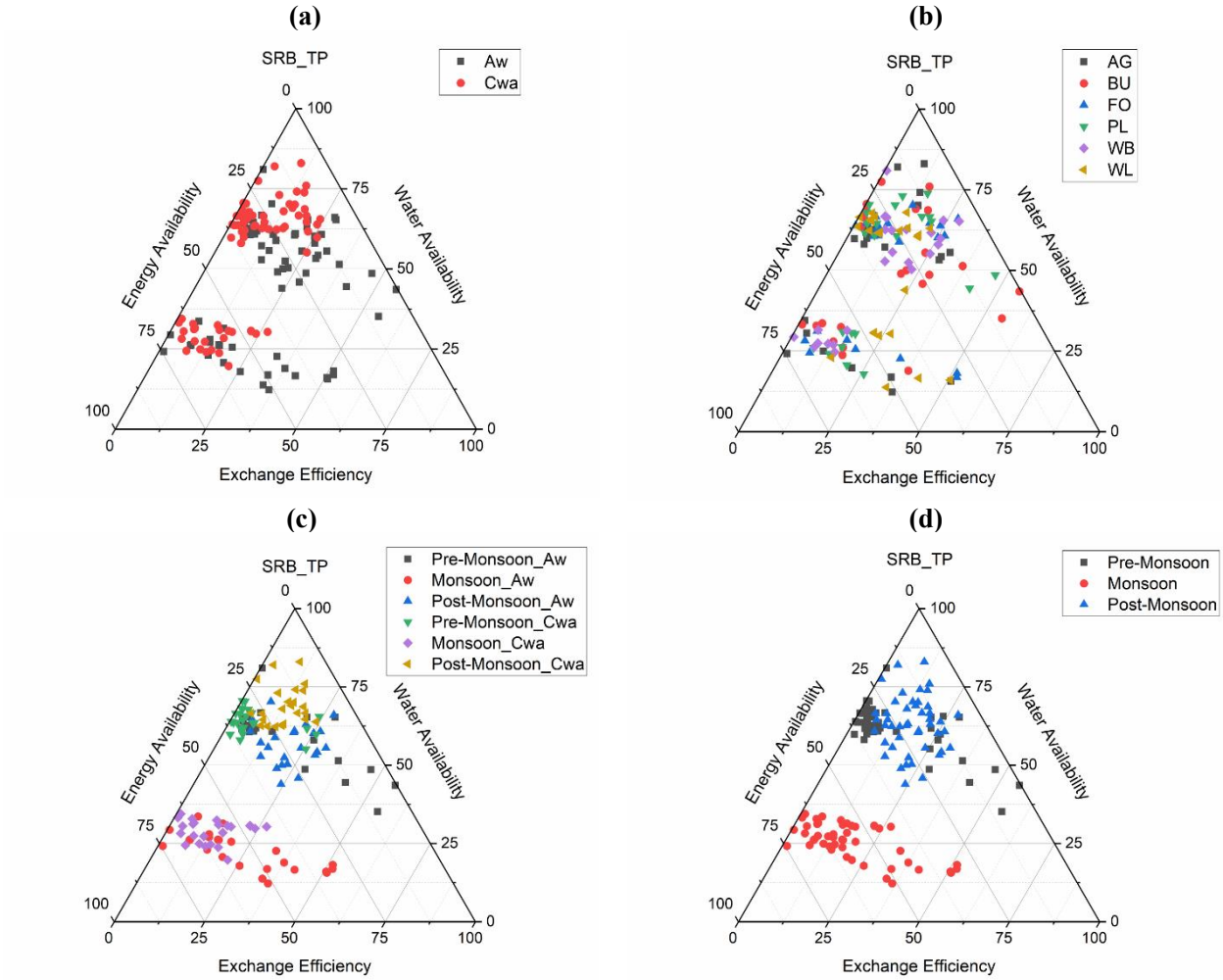

Figure 5: Ternary plot of observed sites for precipitation drivers; according to (a) Climate zone, (b) LULC class, (c) Seasons and Climate zone and (d) Seasons

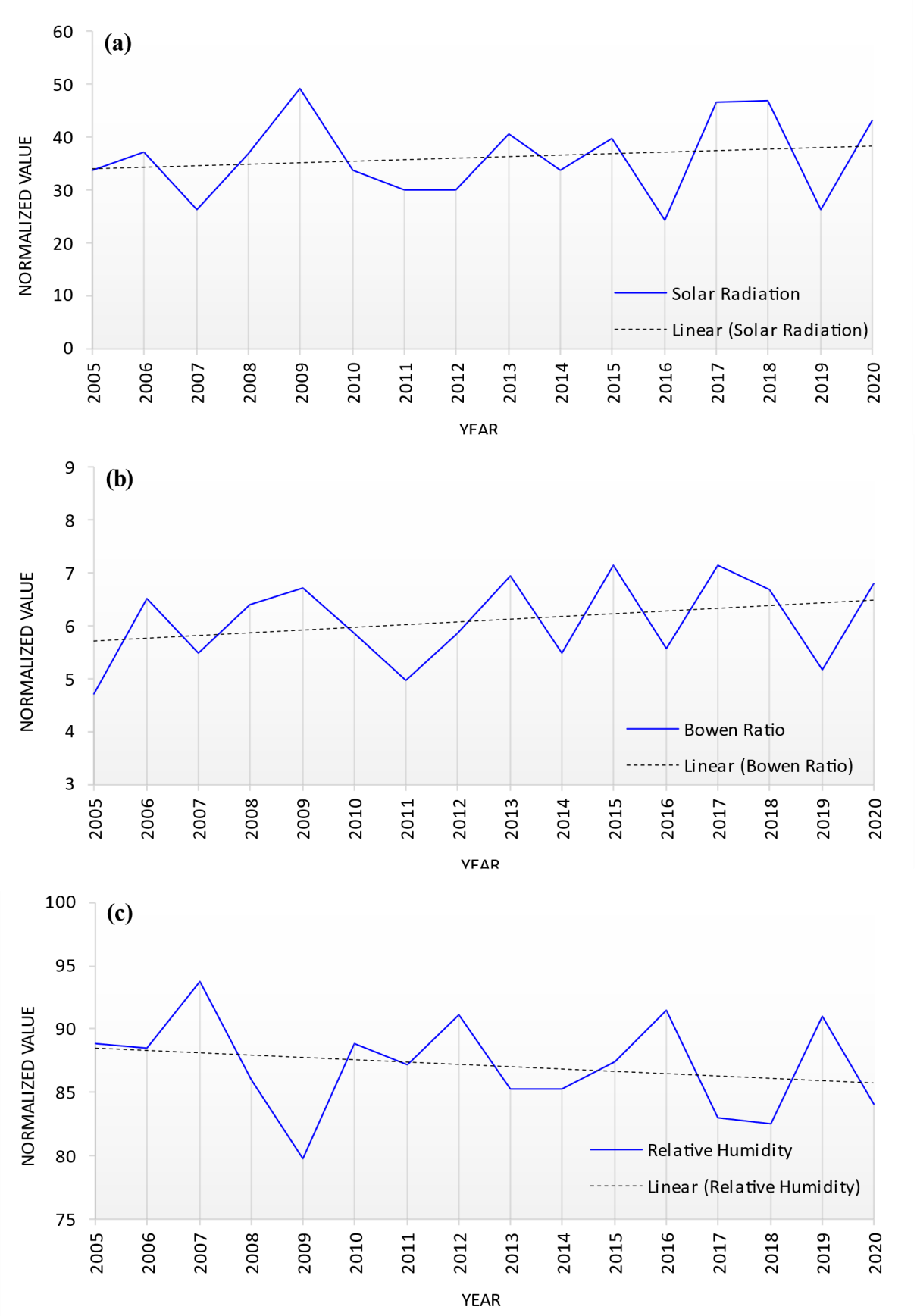

Figure 6: Time series plot and liner trend line; (a) Solar Radiation, (b) Bowen Ratio and (c) Relative Humidity

To grasp climate change at a local scale, it is essential to understand the relationship of heat balance between the ground and the atmosphere. The total radiation received on the earth's surface is allocated into heat that is transferred to

the ground, sensible heat and latent heat. Nonetheless, even when the total radiation reaching the earth's surface remains constant, the temperature and relative humidity in proximity to the surface can fluctuate considerably, depending on the distribution of that radiation between sensible and latent heat.

Acknowledgement

The data sets used in this study are freely accessible from the India Meteorology Department (IMD) (https://mausam.imd.gov.in) and European Centre for Medium-Range Weather Forecasts (ECMWF) (https://cds.climate.copernicus.eu).

References

1. Anand N., Satheesh S.K. and Moorthy K.K., Land-Atmosphere Interactions at a Semi-Arid Region in the Deccan Plateau, *Journal of Geophysical Research: Atmospheres*, **127(21)**, e2022JD037211 **(2022)**

2. Back L.E. and Bretherton C.S., The relationship between wind speed and precipitation in the Pacific ITCZ, *Journal of Climate*, **18(20)**, 4317-4328 **(2005)**

3. Bhimala K.R., Rakesh V., Prasad K.R. and Mohapatra G.N., Identification of vegetation responses to soil moisture, rainfall and LULC over different meteorological subdivisions in India using remote sensing data, *Theoretical and Applied Climatology*, **142(3)**, 987-1001 **(2020)**

4. Biswas A., Jana A. and Mandal A., Application of Remote Sensing, GIS and MIF technique for Elucidation of Groundwater Potential Zones from a part of Orissa coastal tract, Eastern India, *Research Journal of Recent Sciences*, **2**, 42-49 **(2013)**

5. Chakraborty S., Saha U. and Maitra A., Relationship of convective precipitation with atmospheric heat flux — A regression approach over an Indian tropical location, *Atmospheric Research*, **161-162**, 116-124 **(2015)**

6. Das P. et al, Quantification of heat wave occurrences over the Indian region using long-term (1979–2017) daily gridded (0.5° × 0.5°) temperature data — a combined heat wave index approach, *Theoretical and Applied Climatology*, **142**, 497-511 **(2020)**

7. Douglas E.M., Beltrán-Przekurat A., Niyogi D., Pielke R.A. and Vörösmarty C.J., The impact of agricultural intensification and irrigation on land–atmosphere interactions and Indian monsoon precipitation — A mesoscale modeling perspective, *Global and Planetary Change*, **67(1)**, 117-128 **(2009)**

8. Du J., Zhou L., Yu X., Ding Y., Zhang Y., Wu L. and Ao T., Understanding precipitation concentration changes, driving factors and responses to global warming across mainland China, *Journal of Hydrology*, **645**, 132164 **(2024)**

9. Garg V., Aggarwal S.P., Gupta P.K., Nikam B.R., Thakur P.K., Srivastav S.K. and Senthil Kumar A., Assessment of land use land cover change impact on hydrological regime of a basin, *Environmental Earth Sciences*, **76(18)**, 635 **(2017)**

10. Halder S., Saha S.K., Dirmeyer P.A., Chase T.N. and Goswami B.N., Investigating the impact of land-use land-cover change on Indian summer monsoon daily rainfall and temperature during 1951–2005 using a regional climate model, *Hydrol Earth Syst Sci*, **20(5)**, 1765-1784 **(2016)**

11. Jansen F.A., The potential of actual evaporation: A data-driven study of surface evaporation in the Netherlands, Wageningen University and Research **(2023)**

12. Jou Y.J., Huang C.C.L. and Cho H.J., A VIF-based optimization model to alleviate collinearity problems in multiple linear regression, *Computational Statistics*, **29(6)**, 1515-1541 **(2014)**

13. Kim J.H., Multicollinearity and misleading statistical results, *Korean Journal of Anesthesiology*, **72(6)**, 558-569 **(2019)**

14. Kim K.Y., Kim K.R. and Kim H.D., Analysis of time variations in relative humidity around a water area using Bowen ratio, *Journal of Environmental Science International*, **23(10)**, 1731-1743 **(2014)**

15. Kishore P., Jyothi S., Basha G., Rao S.V.B., Rajeevan M., Velicogna I. and Sutterley T.C., Precipitation climatology over India: validation with observations and reanalysis datasets and spatial trends, *Climate Dynamics*, **46(1)**, 541-556 **(2016)**

16. Krishnamurti T.N. and Biswas M.K., Transitions in the surface energy balance during the life cycle of a monsoon season, *Journal of Earth System Science*, **115(2)**, 185-201 **(2006)**

17. Laguë M.M., Bonan G.B. and Swann A.L.S., Separating the Impact of Individual Land Surface Properties on the Terrestrial Surface Energy Budget in both the Coupled and Uncoupled Land–Atmosphere System, *Journal of Climate*, **32(18)**, 5725-5744 **(2019)**

18. Lal P., Shekhar A. and Kumar A., Quantifying Temperature and Precipitation Change Caused by Land Cover Change: A Case Study of India Using the WRF Model, *Frontiers in Environmental Science*, **9**, 1-14 **(2021)**

19. Masroor M., Avtar R., Sajjad H., Choudhari P., Kulimushi L.C., Khedher K.M., Komolafe A.A., Yunus A.P. and Sahu N., Assessing the Influence of Land Use/Land Cover Alteration on Climate Variability: An Analysis in the Aurangabad District of Maharashtra State, India, *Sustainability*, **14(2)**, 642 **(2022)**

20. Prijith S.S., Srinivasarao K., Lima C.B., Gharai B., Rao P.V.N., SeshaSai M.V.R. and Ramana M.V., Effects of land use/land cover alterations on regional meteorology over Northwest India, *Science of The Total Environment*, **765**, 142678 **(2021)**

21. Rajput P. and Sinha M.K., Geospatial evaluation of drought resilience in sub-basins of Mahanadi river in India, *Water Supply*, **20(7)**, 2826-2844 **(2020)**

22. Raman S., Mohanty U.C., Reddy N.C., Alapaty K. and Madala R.V., Numerical Simulation of the Sensitivity of Summer Monsoon Circulation and Rainfall over India to Land Surface Processes, *Pure and Applied Geophysics*, **152(4)**, 781-809 **(1998)**

23. Richardson T., Forster P., Andrews T., Boucher O., Faluvegi G., Fläschner D., Hodnebrog Ø., Kasoar M., Kirkevåg A. and Lamarque J.F., Drivers of precipitation change: An energetic understanding, *Journal of Climate*, **31(23)**, 9641-9657 **(2018)**

24. Sahu J., Sinha M.K., Ghodichore N. and Dewangan S., Study River Dynamics: Backwater Effect in the Upstream of Kelo Dam in Mahanadi River, Chhattisgarh, India, *Advances in River Corridor Research and Applications, Lecture Notes in Civil Engineering*, **470(1)**, 75-89 **(2024)**

25. Sehler R., Li J., Reager J. and Ye H., Investigating Relationship Between Soil Moisture and Precipitation Globally Using Remote Sensing Observations, *Journal of Contemporary Water Research & Education*, **168(1)**, 106-118 **(2019)**

26. Shanmugam K. and Ghosh S., Prediction of daily rainfall state in a river basin using statistical downscaling from GCM output, *Stochastic Environmental Research and Risk Assessment*, **25**, 457-474 **(2011)**

27. Singh P., Kumar V., Thomas T. and Arora M., Changes in rainfall and relative humidity in river basins in northwest and central India, *Hydrological Processes*, **22(16)**, 2982-2992 **(2008)**

28. Sinha M.K., Baier K., Azzam R., Verma M.K. and Kumar S., Impacts of Climate Variability on Urban Rainfall Extremes Using Statistical Analysis of Climatic Variables for Change Detection and Trend Analysis, *Water Resources Management and Sustainability*, **1**, 333-387 **(2022)**

29. Talukdar S., Singha P., Mahato S., Shahfahad, Pal S., Liou Y.A. and Rahman A., Land-Use Land-Cover Classification by Machine Learning Classifiers for Satellite Observations—A Review, *Remote Sensing*, **12(7)**, 1135 **(2020)**

30. Trenberth K.E. and Shea D.J., Relationships between precipitation and surface temperature, *Geophysical Research Letters*, **32(14)**, 1-4 **(2005)**

31. Uyanık G.K. and Güler N., A Study on Multiple Linear Regression Analysis, *Procedia - Social and Behavioral Sciences*, **106**, 234-240 **(2013)**

32. Zheng Y., Kumar A. and Niyogi D., Impacts of land–atmosphere coupling on regional rainfall and convection, *Climate Dynamics*, **44(9)**, 2383-2409 **(2015)**.

(Received 13th November 2024, accepted 17th December 2024)